A CSRR DGS Loaded Dual-Frequency Microstrip Antenna in Ground Plane for Application in PCS and WLAN Communication System

Jyoti Ranjan Panda, Sandeep Kumar Dash, Satya Narayan Mishra, Sambit Prasad Kar

Abstract*: In this paper, a rectangular microstrip antenna which is inset-fed by the microstrip line with a complementary split ring resonator (CSRR) defected ground structure (DGS) cell in the ground plane just below the microstrip line (substrate present in between) for the dual frequency operation at 1.92 GHz and 5.22 GHz is presented, which are the operation bands of personal communication system (PCS) and wireless local area network (WLAN) respectively. The fundamental mode TM_{10} and one strongly activated higher order mode are excited which are responsible for the dual-band operation. Smaller broadside radiation and same polarization planes are the characteristics of these modes.

Keywords: CSRR, DGS, Dual-frequency, inset-fed, PCS, WLAN, rectangular microstrip antenna, wireless communication.

I. INTRODUCTION

In the year 1953, George A. Deschamps [1] proposed the microstrip radiators, which has completely revolutionized the field of antenna theory and techniques. The practical microstrip antennas were first developed by Munson [2] and Howell [3] in the year of 1970. Due to some well known features such as less fragile, low profile, light weight, integrability with monolithic microwave integrated circuits, microstrip antennas are well accepted in the modern wireless communication domain. Narrow bandwidth is the main disadvantage associated with microstrip antenna and it is because of the resonant characteristics of the microstrip patch antenna. But applications like satellite links (vehicular, GPS, etc) as well as emerging applications such as local area networks (WLAN) requires compact and low cost planar antennas. As the microstrip antenna is very light in weight, for the systems which have the airborne platforms, microstrip antennas are suitable candidates such as scatterometers and synthetic aperture radars (SAR). Due to these novel characteristics and applications of the microstrip patch antennas, motivation is generated for the development and research on the fundamental solutions that mitigate the bandwidth limitations of the patch antennas. The two separate sub-bands are the essential for the enhancement of the bandwidth. The broadening of total bandwidth is the alternative approach which can be obtained through the dual band microstrip antenna, which demonstrated this dual resonant behavior in single resonant element.

The introduction of the reactive loading in the radiating element of the inset-fed microstrip antenna is the most well known technique for generation of the dual-frequency behavior in the microstrip antenna. The creation or etching of the slots in the radiating element of the microstrip patch antenna is the easiest way of the generation of the dual-frequency behavior in the microstrip patch antenna. A strong modification of the resonant modes is created by the slot loading in the radiating patch of the microstrip antenna. The slots are configured in such a way that it cut and obstruct the current lines of unperturbed modes. For example in [4], the proposed antenna's radiating element composed of a slot ring of square shaped slot and circular ring slot operating at 2.4 GHz and 5.5 GHz. This microstrip patch antenna [5] has a stacked configuration providing a differential dual-frequency operation which has a radiating element consist of two layers of substrate and connected thorough via holes proving the dual-frequency operation at 2.4 GHz/5.5 GHz for WLAN. By tuning the length [6] of the bar slot and the length of the sides of the patches, this microstrip patch antenna provides the dual-frequency and due polarization operation for WLAN. This antenna [7] consists of two stacked patches which have a square patch at the top and a corner-truncated square-ring patch at the bottom. The two patches are connected each-other by four conducting strips providing the two operating frequency at 1.6 GHz and 2.4 GHz (WLAN). In [8], the proposed antenna consist of an open slot in the ground plane provides an orthogonal path. The slot position is in between the feed arms for realization of an embedded circular polarized band at 2.35 GHz and due to an asymmetric dipole like element, dual band characteristics is achieved. In [9], a half ring structure is used

Revised Manuscript Received on February 01, 2020.

***** Correspondence Author

Jyoti Ranjan Panda*, School of Electronics Engineering, Kalinga Institute of Industrial Technology (Deemed to be University), Bhubaneswar-751024, Odisha, INDIA, Email: jyotiranjan.pandafet@kiit.ac.in

Sandeep Kumar Dash, School of Electronics Engineering, Kalinga Institute of Industrial Technology (Deemed to be University), Bhubaneswar-751024, Odisha, INDIA. Email: sandeepfet@kiit.ac.in

Satya Narayan Mishra, School of Electronics Engineering, Kalinga Institute of Industrial Technology (Deemed to be University), Bhubaneswar-751024, Odisha, INDIA , Country. Email: snmishrafet@kiit.ac.in

Sambit Prasad Kar, School of Electronics Engineering, Kalinga Institute of Industrial Technology (Deemed to be University), Bhubaneswar-751024, Odisha, INDIA. Email: spkarfet@kiit.ac.in

for generation of the dual-frequency operation along with a half circular patch at 0.9 GHz and 1.8 GHz which is applicable for PCS application. In [10], various low profile, compact, wideband microstrip patch antenna designs are provided which are based on co-directional complementary SRRs. In [11], the dual-frequency and dual polarization is achieved by the two triangular rings in this microstrip antenna. In [12], a via loaded ring is present on the bottom layer in this antenna and in top layer a circular patch is present. The two patches are coupled fed by the circular coupler provides dual-band operation at 2.41 GHz and 5.5 GHz which are the operation band of WLAN. In [13], generation of two identical polarizations and dual-frequency operation are accomplished by using the two elements formed by the single feed-line. This microstrip antenna provides the dual-frequency operation at 3.9 GHz and 4.9 GHz. In [14], additional resonant modes and dual-frequency operation are induced by the introduction of symmetrical slots at the edges of the rectangular patch. In [15], a half E-shaped microstrip patch antenna (HEMSPA) which provides three dual-bands with dual sense polarization. Four T-slits are etched out in the radiating edges of HEMSPA.

In this paper, an inset-fed simple dual-frequency rectangular microstrip antenna is proposed, based on the several different dual-frequency a microstrip antenna structures which is loaded with loaded with a CSRR DGS cell in the ground plane and it is just beneath the microstrip feed-line (substrate is present in between).The proposed antenna exhibits dual-frequency operation and it is achieved by creating a CSRR DGS cell in the ground plane of the inset-fed rectangular microstrip antenna. A 50-Ω microstrip transmission line is used as the feeding structure for the proposed microstrip antenna and feeding microstrip transmission line is inserted into the radiating element of the rectangular radiating element for appropriate impedance matching. The inset-fed rectangular dual-frequency microstrip antenna which is proposed in this manuscript resonates at 1.92 GHz (TM_{10}Mode) and 5.22 GHz (a strong higher order mode) which have the percentage bandwidth of 3.65 and 2.49 GHz respectively. The characteristic of the CSRR DGS cell is studied and the represented by its equivalent circuit. The parameters of the equivalent circuit are extracted by the curve fitting and the parameter extraction method. Since one of the resonant frequencies is at 1.92 and 5.22 GHz, the proposed dul-frequency microstrip antenna can be appropriately applicable in the operation band of personal communication system (PCS) and wireless local area network (WLAN).

In this paper, an inset-microstrip-line-fed rectangular microstrip antenna loaded with a CSRR DGS cell in the ground plane just beneath the microstrip feed-line (substrate is present in between) for the dual-frequency operation is proposed. The proposed dual-frequency inset-fed rectangular microstrip antenna exhibit resonance at 1.92 GHz and 5.22 GHz which are the operation bands of personal communication system (PCS) and wireless local area network (WLAN) respectively.

II. ANTENNA DESIGN AND RESULTS

A. Single Frequency inset-fed Rectangular Microstrip Antenna

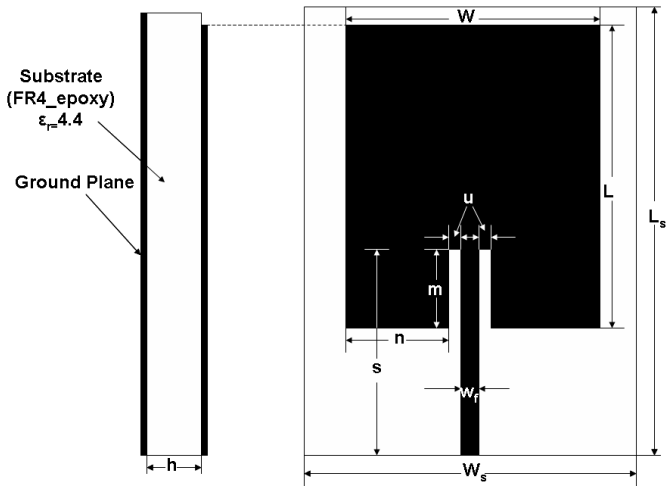

Fig. 1. Geometry of antenna 1.

A single frequency inset-fed rectangular microstrip antenna's geometry and configuration is shown in the Fig. 1. The antenna (referred as the antenna 1) is simulated on the substrate of FR4 epoxy which has the dielectric constant of ε_r=4.4 and height of h=1.6 mm, which has the loss tangent of tanδ=0.02. The proposed microstrip antenna is fed by 50-Ω microstrip transmission line as shown in the Fig. 1. For the appropriate impedance matching the microstrip line feed is inserted deep into the rectangular radiating element. This category of feeding the microstrip antenna is known as the "inset-feeding". For simulation and optimization purpose of the proposed inset-fed microstrip antenna, full wave finite element method (FEM) based electromagnetic software of HFSS V14 [18] is employed. The design parameters are W_s=50 mm, L_s=75 mm, W= 25 mm, L=38 mm, m =14 mm, n=9.925 mm, u =1.05 mm and w_f=3.05 mm.

The fundamental resonant frequency $(f_r)_m$ (subscript m for microstrip antenna) of the inset-fed rectangular microstrip antenna is given by [16]

$$(f_r)_m = \frac{c_0}{2W\sqrt{\frac{2}{\varepsilon_r+1}}} \quad (1)$$

Since L>W>h, the first resonance is due to the dominant mode of the rectangular microstrip antenna which is TM_{10} mode. For the dominant mode TM_{10}, the expression for the resonant frequency is given by [16]

$$(f_r)_{TM_{10}} = \frac{c_0}{2L\sqrt{\varepsilon_r}} \quad (2)$$

where c_0 is the free space velocity of light, L inset-fed rectangular microstrip antenna length, ε_r substrate dielectric constant of the proposed antenna. Patch resembles larger than the normal rectangular patch due to the fringing and the length correction factor is employed to tackle the length enlargement of the patch due to fringing. The effective length L_{eff} is used for the length correction in place of the actual length which is given by [17]

$$L_{eff} = L + 2\Delta L \quad (3)$$

where

$$\Delta L=0.412h[\frac{(\varepsilon_{reff}+0.3)(\frac{W}{h}+0.264)}{(\varepsilon_{reff}-0.258)(\frac{W}{h}+0.8)}] \quad (4)$$

where

$$\varepsilon_{reff}=\frac{\varepsilon_r+1}{2}+\frac{\varepsilon_r-1}{2}[1+12\frac{h}{W}]^{-\frac{1}{2}} \quad (5)$$

where h is dielectric substrate's height. After length correction, the dominant mode TM_{10}'s resonant frequency is modified by eq. (3) and is given by

$$(f_r)_{TM_{10}}=\frac{c_0}{2L_{eff}\sqrt{\varepsilon_r}} \quad (6)$$

Hence, applying all the numerical values of the design parameters into eq.(1) to eq.(6), the theoretical fundamental resonant frequency$(f_r)_m$ and resonance frequency of the first dominant mode (TM_{10}) were found to be 1.81 GHz and 3.65 GHz respectively.

The inset-fed rectangular microstrip antenna's (antenna 1) return loss (reflection coefficient) versus frequency graph is shown in the Fig. 2. The resonances for the antenna 1 occur at 1.92 GHz (TM_{10} mode) and 3.61 GHz having the return loss of –19.23 dB and -36.24 respectively. The first resonance frequency ($(f_r)_{TM10}$) 1.92 GHz is due to the dominant mode TM_{10}, which is somewhat closer to it's theoretical value of 1.81 GHz. The second resonant frequency (3.61 GHz) is the fundamental resonant frequency $(f_r)_m$, which is very closer to it's theoretical value (3.65 GHz) derived from the eq.(1). The percentage bandwidth at the two resonant frequencies of 1.92 GHz and 3.61 GHz are 3.65 and 2.49 respectively.

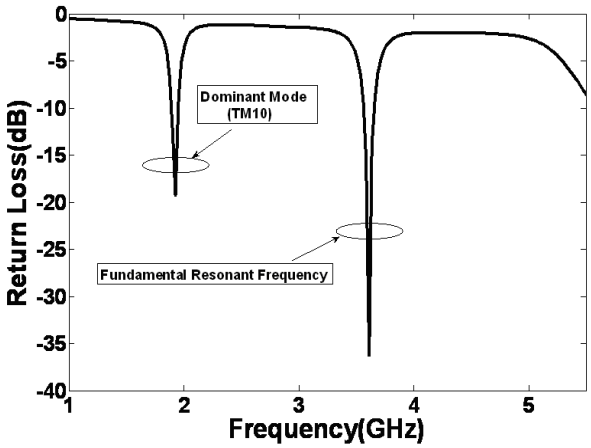

Fig. 2. Return Loss (dB) vs. frequency of antenna 1.

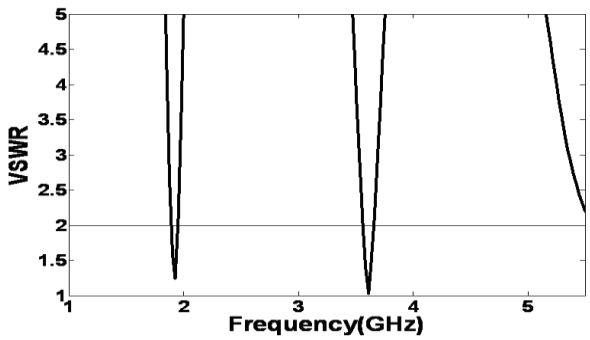

Fig. 3. VSWR vs. frequency of antenna 1.

A characteristic of VSWR of the antenna 1 is provided in the Fig. 3. The VSWR of the antenna 1 is extended from 1.88 GHz to 1.95 GHz which has the resonant frequency centered at 1.92 GHz which is due to the dominant mode TM_{10}. The value of VSWR at the first resonance frequency of 1.92 GHz is 1.24. Similarly the VSWR graph cuts the VSWR=2 line at 3.56 GHz and remains below the line till 3.65 GHz at the fundamental resonant frequency of 3.61 GHz. The value of VSWR at the fundamental resonance frequency of 3.61 GHz is 1.03.

From the Fig. 4 the inset-fed rectangular microstrip antenna's variation of the input impedance versus frequency can be seen. At 1.92 GHz and 3.61 GHz, the values of imaginary part (reactance) of the input impedance are almost 0-Ω and simultaneously the value of real part (resistance) is approximately 50-Ω.

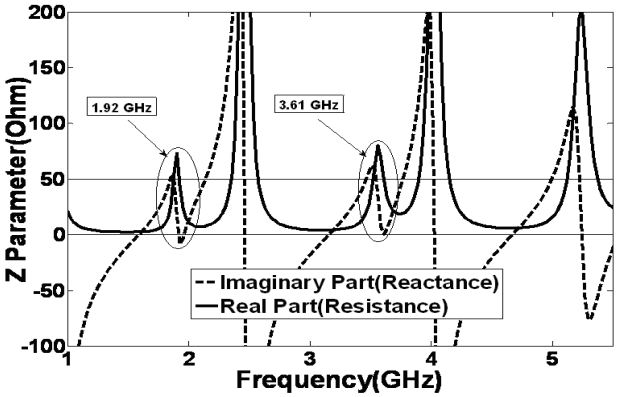

Fig. 4. Z parameter vs. frequency of antenna 1.

B. Complementary Split Ring Resonator (CSRR) defected ground structure (DGS) Characterization

The defected ground structure (DGS) was first reported by Park et al, which is based on the photonic band gap (PBG) structure [19] in the year 1999. The DGS structures can be used in planar microwave circuits to develop the low-pass filers [20-21].

The DGSs can be realized by creating defects in the ground plane of planar circuits. In other words, some portion of the ground plane is etched out of a definite shape to provide the disturbance in the current distribution in the ground plane. Hence the DGS has the great merit towards the compact structure, small size as well as the filter design on the basis of the equivalent circuit and the parameter extraction technique.

In recent times the complementary split ring resonator (CSRR) DGS has gain the widespread acceptance towards the efficient defected ground structure [22-23], which generates a transmission zero at the out-of-band. Due to this property of CSRR DGS, filter design can be possible with much steeper slope. The CSRR DGS is comprised of two concentric split rings of different size and inverse split direction. This CSRR DGS structure is removed from the ground plane of the planar structure consist of a misrostrip transmission line. The structure of the CSRR DGS cell is shown in Fig. 5. The substrate is made up of FR4-epoxy of dielectric constant ε_r=4.4 and the thickness of the substrate is h=1.6 mm.

The dimensions of CSRR DGS are given as a=8.0 mm, g=c=t=0.5 mm and w_f=3.05 mm.

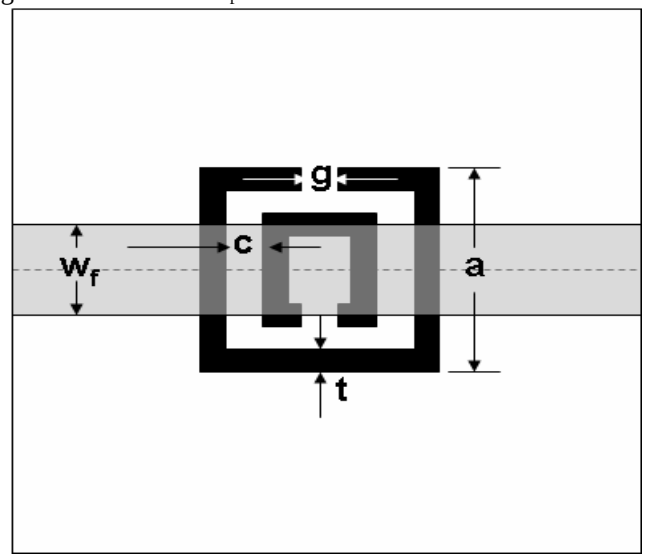

Fig.5. Structure of single CRSS DGS cell.

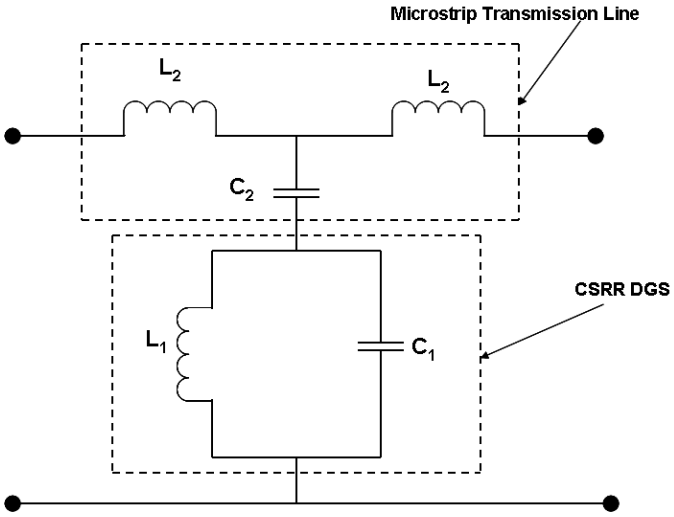

Fig.6. Equivalent circuit of a single CSRR DGS cell.

The equivalent circuit of s single CSRR DGS cell is shown in the Fig.6.A 50-Ω microstrip transmission line, which is comprised of two series inductors and s shunt capacitor and CSRR forms a parallel resonant circuit. Hence removing a split ring defective pattern from the ground plane adds a parallel resonant circuit equivalent to the equivalent RHTL. The location of the transmission zero for the CSRR DGS can be determined by the resonant frequency of the shunt circuit that means it is codetermined by L_1, C_1 and C_2.The parallel LC circuit impedance is given by

$$Z_1 = \frac{1}{j\omega C_1 + \frac{1}{j\omega L_1}} = j\frac{\omega L_1}{1-\omega^2 L_1 C_1} \quad (7)$$

while the impedance of the single capacitor is given by

$$Z_2 = \frac{1}{j\omega C_2} = -j\frac{1}{\omega C_2} \quad (8)$$

The transmission zero is obtained when

$$Z_1 + Z_2 = 0 \quad (9)$$

Then the resonant frequency of the CSRR DGS is given as

$$f_s = \frac{1}{2\pi\sqrt{L_1(C_1+C_2)}} \quad (10)$$

Fig. 7 depicts the simulated scattering parameters of the single CSRR DGS cell. The resonant frequency f_s of the single CSRR DGS cell can be found out from the S_{21} parameter shown in the Fig.7 and the value of the resonant frequency f_s is 2.40 GHz at -17.59 dB S_{21} parameter value. The 3-dB cut-off frequency can be calculated from the graph of S_{21} parameter and it was found to be 2.31 GHz.

Fig. 8(a) shows the variation of the resonant frequency (f_s) with the variation of the outer length "a" of the CSRR DGS., when all the other parameters such as c=g=0.5 mm are kept constant. When the outer length "a" is increased from 8 mm to 11 mm, the resonant frequency (f_s) shifts towards left i.e. the resonant frequency (f_s) decreases with the increase of the outer length "a" of the CSRR DGS. The reason behind this characteristic of the CSRR DGS is, when the outer length of the CSRR DGS is increased, the effective inductance L_1 is increased, which lowers the resonant frequency (f_s). Similarly Fig. 8(b) shows the variation of the resonant frequency (f_s) with the variation of the outer length "g" of the CSRR DGS, when all the other parameters such as a=8.0 mm and c=0.5 mm are kept constant. When the outer length "g" is increased from 0.5 mm to 2.5 mm, the resonant frequency (f_s) shifts towards right i.e. the resonant frequency (f_s) increases with the increase of the outer length "a" of the CSRR DGS. From the Fig.8(c), it is clear that when the gap "c" between the outer ring and the inner ring of the CSRR DGS is increased from 0.5 mm to 2.5 mm, when all the other parameters such as a=8.0 mm and g=0.5 mm are kept constant, the resonant frequency (f_s) shifts towards left i.e. the resonant frequency (f_s) decreases with the increase of the outer length "c" of the CSRR DGS.

With the design parameters a=8.0 mm, g=c=t=0.5 mm and w_f=3.05 mm
of the single CSRR DGS and with the help of the curve fitting and parameter extraction method, the corresponding equivalent circuit values of the CSRR DGS can be determined and they are given by L_1=3.176 nH, C_1=0.528 pF, C_2=0.718 pF and L_2=2.85 nH. Fig.9 shows the graph of simulated scattering parameters of the single CSRR DGS cell compared with the scattering parameters generated by the equivalent circuit method. From the graph it is clear that there is slight discrepancy between the simulated scattering parameter and that generated from the curve fitting and parameter extraction method of the single CSRR DGS cell.

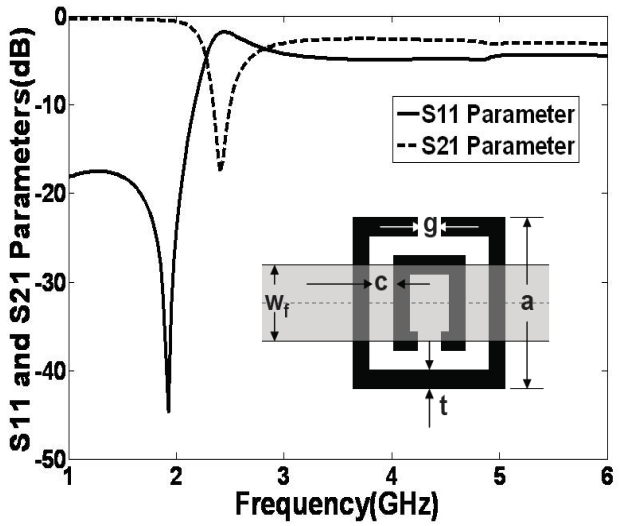

Fig. 7. Simulated scattering parameters of the single CSRR DGS cell.

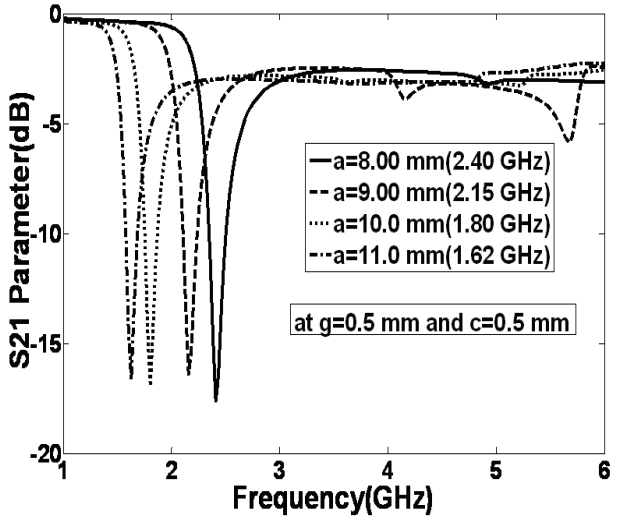

(a)

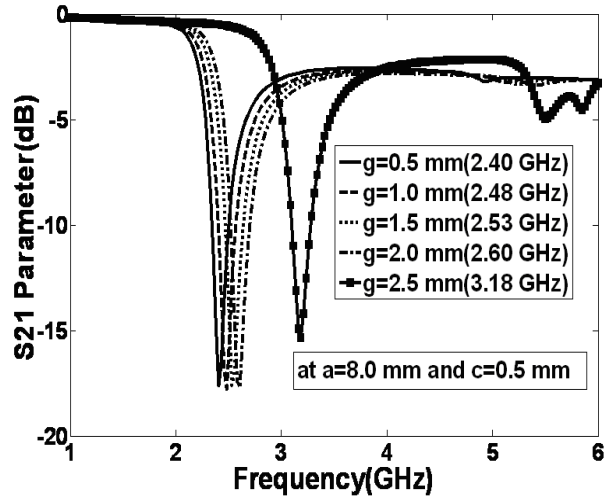

(b)

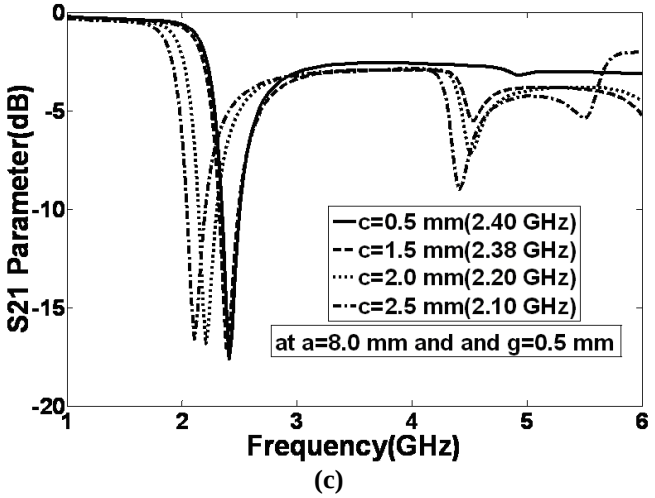

(c)

Fig.8. (a) Simulated S_{21}-parameter (dB) of the single CSRR DGS cell with the variation of a when g=c=0.5 mm, (a) with the variation of g when a=8.0 mm and c=0.5 mm, (c) with the variation of c when a=8.0 mm and g=0.5 mm.

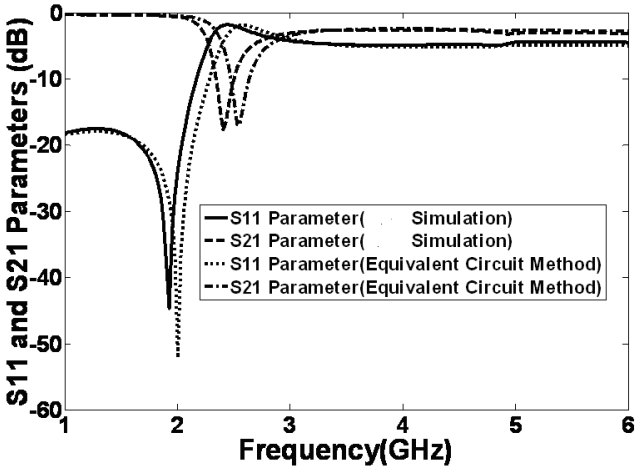

Fig.9. Simulated scattering parameters of the single CSRR DGS cell compared with the scattering parameters generated by the equivalent circuit method.

C. Dual-frequency inset-fed rectangular microstrip antenna loaded with a CSRR DGS cell in the ground plane.

The dimension and geometry of the dual-frequency inset-fed microstrip antenna is shown in Fig. 10, which is loaded with a CSRR DGS cell (referred to as antenna 2 in this paper) in the ground plane and it is just beneath the microstrip feed-line (substrate is present in between) of the proposed rectangular mucrostrip antenna. The design parameters of antenna 2 given by are W_s=50 mm, L_s=75 mm, W= 25 mm, L=38 mm, m =14 mm, n=9.925 mm, u =1.05 mm, s=50 mm, p=22 mm, a=8.0 mm, g=c=t=0.5 mm and w_f=3.05 mm.

The return loss (dB) vs. frequency of the dual frequency inset-fed rectangular microstrip antenna shown in Fig. 11

loaded with a CSRR DGS in the ground plane beneath the microstrip feed-line(substrate is present in between).

The antenna 2 resonates at three different frequencies among which there are two prominent resonances at 1.92 GHz at the return loss of -21.19 dB and 5.22 GHz at the return loss value of -21.28 dB. The two resonances at 1.92 GHz and 5.22 GHz are the operating frequencies for the PCS/GSM and the WLAN. That's why this proposed antenna finds application in the wireless communication domain. The percentage bandwidth at the two resonant frequencies of 1.92 GHz and 5.22 GHz are 3.65 and 2.49 respectively.

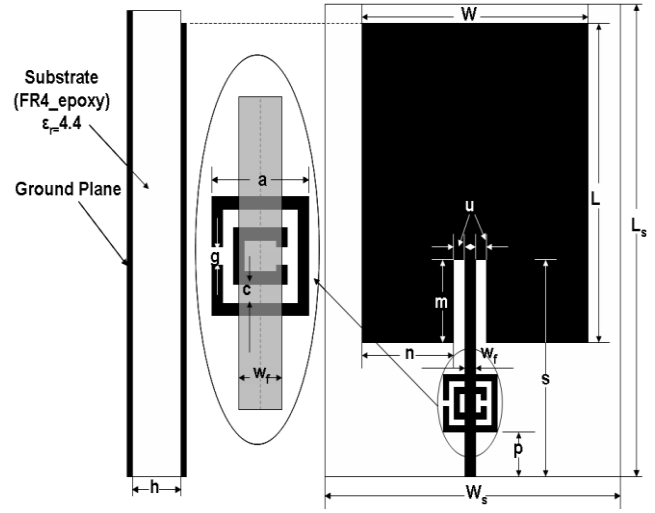

Fig. 10. Geometry of antenna 2.

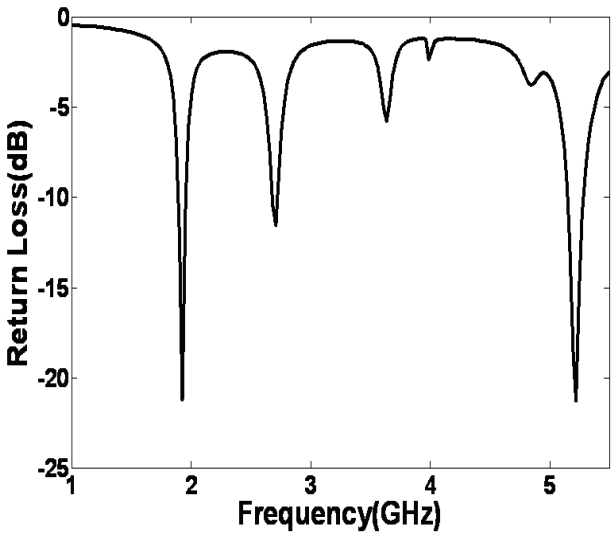

Fig. 11. Return loss (dB) vs. frequency of antenna 2 at W_s=50 mm, L_s=75 mm, W= 25 mm, L=38 mm, m =14 mm, n=9.925 mm, u =1.05 mm, s=50 mm, p=22 mm, a=8.0 mm, g=c=t=0.5 mm and w_f=3.05 mm.

A characteristic of VSWR of the antenna 2 is provided in the Fig. 12. The VSWR of the antenna 2 is extended from 1.88 GHz to 1.95 GHz which has the resonant frequency centered at 1.92 GHz which is due to the dominant mode TM_{10}. The value of VSWR at the first resonance frequency of 1.92 GHz is 1.19. Similarly the VSWR graph cuts the VSWR=2 line at 5.15 GHz and remains below the line till 5.28 GHz at third resonant frequency of 5.22 GHz. The value of VSWR at the third resonance frequency of 5.22 GHz is 1.18.

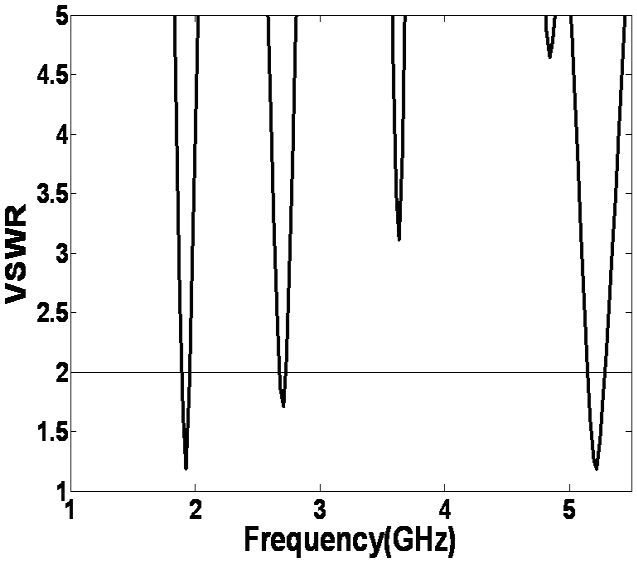

Fig. 12. Simulated VSWR vs. frequency of antenna 2 at W_s=50 mm, L_s=75 mm, W= 25 mm, L=38 mm, m =14 mm, n=9.925 mm, u =1.05 mm, s=50 mm, p=22 mm, a=8.0 mm, g=c=t=0.5 mm and w_f=3.05 mm.

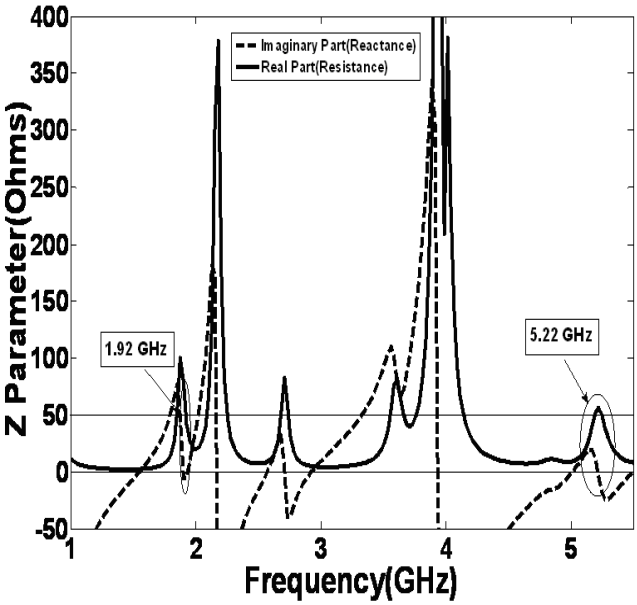

Fig. 13. Z parameter vs. frequency of antenna 2 at W_s=50 mm, L_s=75 mm, W= 25 mm, L=38 mm, m =14 mm, n=9.925 mm, u =1.05 mm, s=50 mm, p=22 mm, a=8.0 mm, g=c=t=0.5 mm and w_f=3.05mm.

From the Fig. 13 the variation of the input impedance versus frequency of antenna 2 can be seen. At 1.92 GHz, the value of the input reactance is almost 0-Ω, which is the imaginary part of the input impedance and simultaneously the value of the input resistance is almost 50-Ω, which is the real part of the input impedance. The same situation prevails at the second resonance frequency of 5.22 GHz. Hence from Fig. 13 it is clear that the first resonant frequency (1.2 GHz) as well as the second resonant frequency (5.22 GHz), the proper impedance matching occurs for the proposed inset-fed dual-frequency microstrip patch antenna.

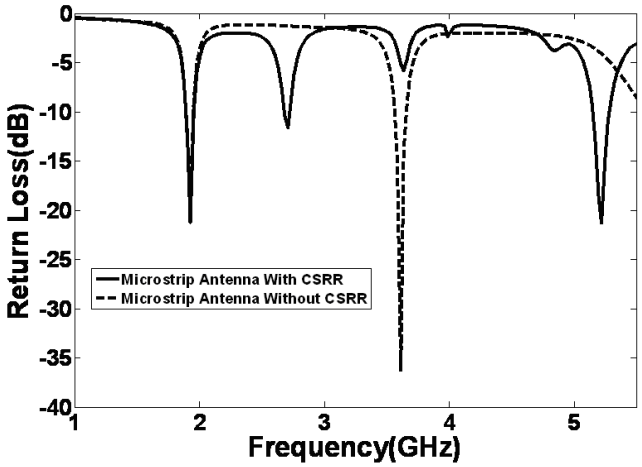

Fig. 14. Simulated return loss of the microstrip antenna without CSRR DGS compared with the simulated return loss of the microstrip antenna without CSRR DGS.

Fig.14 represents the comparison between the simulated return loss of the inset-fed rectangular microstrip antenna with and without CSRR DGS. Without the CSRR DGS cell, inset-fed rectangular microstrip antenna resonates at 1.92 GHz and 3.61 GHz. The resonance at 3.61 GHz is the fundamental resonance frequency of the microstrip antenna without CSRR DGS and the second resonance frequency at 1.92 GHz is due to the activation of the dominant mode TM_{10}. When a single CSRR DGS cell is introduced in the ground just below the microstrip ground plane (substrate is present in between), the antenna behaves strangely. The resonant frequency at 1.92 GHz due to the dominant mode TM_{10} is remain unchanged but the fundamental frequency at 3.61 GHz is completely wiped out and in the same time two other higher order modes are activated on the two sides of the fundamental resonance frequency of 3.61 GHz. The new activated higher modes resonate at 2.70 GHz and 5.22 GHz respectively. Among the two new higher order modes, one is weakly activated i.e. at 2.70 GHz and the other mode at 5.22 GHz is strongly activated. The higher order mode at 5.22 GHz enables antenna 2 to operate in the frequency band of WLAN and the dominant mode at 1.92 GHz is the band of operation for the PCS/GSM systems. In this way introducing a CSRR DGS cell in the ground plane of antenna 1 transforms the antenna to resonate strongly at 1.92 GHz and 5.22 GHz and this enables the antenna 2 to be applicable in the wireless (PCS/GSM, WLAN) communication system domain.

In Fig.15, the proposed dual-frequency microstrip antenna's (antenna 2) E-plane (YZ plane) and H-plane (XZ plane) at frequency of 1.92 GHz are depicted. Similarly Fig. 16 shows the proposed antenna 2's E-plane (YZ plane) and H-plane (XZ plane) at frequency of 5.22 GHz. From Fig. 15 and Fig.16, the proposed microstrip antenna's (antenna 2) E-plane (YZ plane) radiation pattern is slightly broader than the H-plane (XZ plane) radiation pattern, which is the general case for the conventional microstrip patch antenna. Same polarization and broadside radiation pattern can be observed at both the operating modes in the proposed antenna (antenna 2).

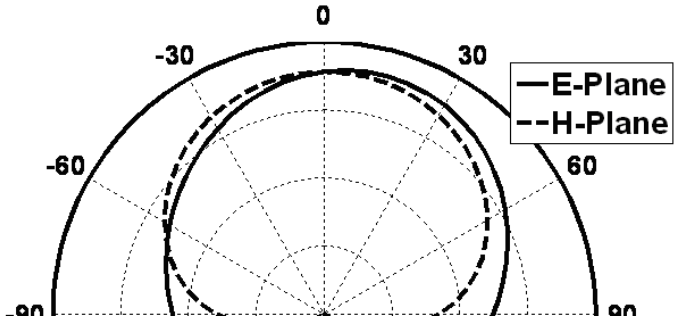

Fig. 15. Antenna 2's simulated E-plane (YZ pane) and H-plane (XY plane) radiation patterns at 1.92 GHz.

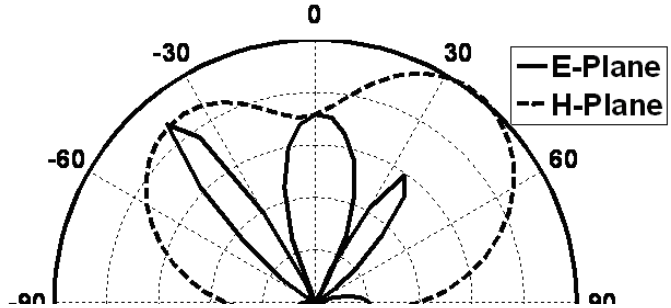

Fig. 16. Antenna 2's simulated E-plane (YZ pane) and H-plane (XY plane) radiation patterns at 5.22 GHz.

III. CONCLUSION

An inset-microstrip-line-fed dual-frequency rectangular microstrip antenna loaded with a CSRR DGS cell in the ground plane just beneath of the microstrip feed-line (substrate is present in between)for application in wireless application such as personal communication system (PCS) (1.92 GHz, fundamental mode TM_{10}) and wireless local area network (WLAN) (5.22 GHz, activated by the CSRR DGS at ground plane) has been demonstrated. The polarization pane is same for the two operating frequencies and similar broadside characteristics are exhibited by the proposed antenna. Hence the proposed microstrip antenna is an excellent candidate for the application as the base stations antennas for wireless communication systems.

REFERENCES

1. G.A. Deschamps,"Microstrip Microwave Antennas," 3rd USAF Symposium on Antennas, 1953.
2. R.E. Munson, "Conformal microstrip antennas and microstrip phased arrays," IEEE Trans. Antennas Propagation., vol. AP-22, no.1, pp.74-78, Jan.1974.
3. J.Q.Howell,"Microstrip Antennas," IEEE Trans. Antennas Propagation., vol. AP-23, no.1, pp.90-93, Jan.1975.
4. W. Ren, "Compact dual-band slot antenna for 2.5/5 GHz WLAN application" Progress in Electromagnetics Research B, vol. 8, pp. 319-327, 2008.
5. L. Han, W. Zhang, X. Chen, G. Han and R. Ma, "Design of compact differential dual-frequency antenna with stacked patches" IEEE Trans. Antennas Propag., vol. 58, no. 4, pp. 1387-1392, Apr. 2010.
6. C.H. Chen, X.L. Wang and W. Wu, "Compact single-feed dual-frequency dual-polarisation microstrip antenna", Electron. lett, vol. 46, no. 20, pp. 1362-1363, Sep. 2010.
7. S. –L. Ma and J. –S. Row, "Design of a single-feed dual frequency patch antenna for GPS and WLAN application" IEEE Trans. Antennas Propag., vol. 59, no. 9, pp. 3433-3436, Sep. 2011.

8. K. L. Bao and M. J. Amman, "Wideband dual frequency dual-polarized dipole like antenna" IEEE Antennas Wireless Propag. Lett., vol. 10, pp. 831–834, 2011.
9. X. Hu, Y. Li, W. Chen, H. –Z. Ta and Y. Long, "Novel dual-frequency microstrip antenna with narrow half-ring and half-circular patch" IEEE Antennas Wireless Propag. Lett., vol. 12, pp. 3–6, 2013.
10. M. –C. Tang, S. Xiao, T. Deng, H. Zhu and B. –Z. Wang, "Design of compact, low profile, wideband, dual-frequency patch antennas based on complementary co-directional SRRs", IEEE Antennas Propagation Magazine, vo. 56, no. 6, pp. 72-89, Dec. 2014.
11. T. Zhang, W. Hong and K. Wu, "A low-profile tripe band triple polarization antenna with two triangular rings", IEEE Antennas Wireless Propag. Lett., vol. 14, pp. 378–381, 2015.
12. Z. Zhang, J. Lin, Y. Li and Y. Long,"A dual-frequency broadband design of coupled-fed stacked microstrip monopolar patch antenna for WLAN application" IEEE Antennas Wireless Propag. Lett., vol. 15, pp. 1289–1292, 2016.
13. S. Chakraborty, "A compact dual frequency microstrip antenna" International Journal of RF and Microwave Computer-aided Engineering, vol. 28, no. 6, pp. 1-10, Mar. 2018.
14. J. Deng and L. Fang, "Dual-band microstrip filtering antenna with symmetrical slots" Progress in Electromagnetic Research Letters, vol. 86, pp. 13-19, 2019.
15. B. Anantha and R. S. R Gosula, "Compact single feed dual band microstrip antenna with adjustable dual circular polarization" IETE Journal of Research, pp. 1-9, 2019.
16. C. A. Balanis, Antenna Theory: Analysis and Design, 3/e, Hoboken, New Jersey: John-Wiley and Sons, 2005.
17. E.O. Hammerstad,"Equations for Microstrip Circuit Design," Proc. Fifth European Microwave Conf., pp.268-272, Sep. 1975.
18. HFSS version 14, Ansoft, USA.
19. J. –I. Park, "Modeling of a photonic bandgap and its application for low-pass filter design," Asia Pacific Microwave Conference, Singapore, pp. 331-334, 1999.
20. C. –S. Kim, J.-I. Park, A. Dal and J. –B. Lim, "A novel 1-D periodic defected ground structure for planar circuits," IEEE Microw. Guided Wave Lett., vol. 10, no. 4, pp. 131-133, Apr 2000.
21. J.-S. Park, J. Kim, J. Lee and S. Myung, " A novel equivalent circuit and modeling method for defected ground structure and its application to optimization of a DGS lowpass filter," IEEE Microwave Theory Tech. Symp. Dig., Seattle WA, pp.417-420, 2002.
22. J. Bonache, F. Martin, F. Falcone, J. D. Baena, T. Lopetegi, J. Garcia-Garcia, M. A.G. Laso, I. Gil, A. Marcotegui, R. Marques and M. Sorolla, "Application of complementary split-ring resonators to the design of compact narrow band-pass structures in the microstrip technology," Microw, Opt Technol Lett., vol.46, no.5, pp.508-512, Sep 2005.
23. Bonache, J., F. Martin, I. Gil, and J. Garcia-Garcia, "Novel microstrip filters based on complementary split rings resonators," IEEE Trans. Microw. Theory Tech., Vol. 54, No. 1, pp. 265-271, Jan 2006.

AUTHORS PROFILE

Jyoti Ranjan Panda, Jyoti Ranjan Panda was born in Bhubaneswar, Odisha, India. He is currently working as Associate Professor in KIIT, Bhubaneswar. His research interest is in Microwave Engineering, planar antennas for wireless communication. Now he is started working also in the field of adaptive and array signal processing. He is a member of IEEE Antennas and Propagation Society and IEEE Microwave Theory and Techniques Society.

Sandeep Kumar Dash Sandeep Kumar Dash was born in Bhubaneswar, Odisha, India. He is currently working as Assistant professor in KIIT, Bhubaneswar. His primary field of work includes analog and mixed signal design and Antenna and Microwave Engineering.

Satya Narayan Mishra Satya Narayan Mishra was born in Bhubaneswar, Odisha, India. He is currently working as Assistant Professor in KIIT, Bhubaneswar. His primary field of work includes Device modelling, analog and mixed signal design and Antenna and Microwave Engineering.

Sambit Prasad Kar Sambit Prasad Kar was born in Bhubaneswar, Odisha, India. He is currently working as Assistant Professor in KIIT, Bhubaneswar. His primary field of research includes Signal Processing and Antenna and Microwave Engineering